2D Pyrene-based Metal−Organic Framework Nanobelts as Efficient Photocatalysts for Coupling of Thiols into Disulfides

Xin Zhao,[a] Yajun Zhao,[a] Tao He, [c] Jing-Tong Deng,[c] Zong-Wen Mo,[a] Jiewei Liu*[a,b]

[a]*School of Environmental and chemical Engineering, Jiangmen Key Laboratory of Synthetic Chemistry and Cleaner Production, Wuyi University, Jiangmen 529020, P.R. China.*

[b]*Institute of Carbon Peaking and Carbon Neutralization, Wuyi University, Jiangmen 529020, P.R. China*

[c]*School of Pharmacy and Food Engineering, Wuyi University, Jiangmen 529020, P.R. China.*

E-mail addresses: wyuchemliujw@126.com

Contents

Captions for Figures and Tables

Figure S1. Optical microscope image of single crystalline Ni-PTTB.

Figure S2. The FT-IR spectra of H_4PTTB and Ni-PTTB.

Figure S3. (a) The coordination mode of the Cd atom in Ni-PTTB; (b) The layered structure of Ni-PTTB with interlayer distance of 10 Å. Color representation: O (red); C (Tan); Cd (Turquoise). H atoms are removed for clarity. The crystal structures of Ni-PTTB viewed along the a axis (c) and c axis (d), respectively (the external and internal pore surfaces are shown in blue).

Figure S4. SEM (a) and EDS mapping images (b) of Ni-PTTB.

Figure S5. The TG curves of activated Ni-PTTB samples.

Figure S6. Stability test of Ni-PTTB in different solvents for 5 days.

Figure S7. Stability test of Ni-PTTB in aqueous solutions with a pH range from 2 to 12 for 5 days.

Figure S8. Schematic of synthetic route of Ni-PTTB and Ni-PTTB-NB nanobelt.

Figure S9. SEM image of 2D Ni-PTTB-NB.

Figure S10. High resolution XPS spectra of Ni 2p in 2D Ni-PTTB-NB.

Figure S11. Open-circuit potential as a function of time under visible light for Ni-PTTB and Ni-PTTB-NB.

Figure S12. The recycling experiment of 2D Ni-PTTB-NB for the photocatalytic coupling of thiols to disulfide.

Figure S13. The PXRD patterns of 2D Ni-PTTB-NB before and after photocatalytic reaction.

Figure S14. The TEM images of 2D Ni-PTTB-NB after photocatalytic reaction.

Figure S15. XPS spectrum of 2D Ni-PTTB-NB after catalytic reaction.

Figure S16. Trapping of thiyl radical-TEMPO adduct measured by GC-MS.

Figure S17. GC trace for the photocatalytic coupling of 4-methoxythiophenol.

Figure S18. GC trace for the photocatalytic coupling of 3-methoxythiophenol.

Figure S19. GC trace for the photocatalytic coupling of 2-methoxythiophenol.

Figure S20. GC trace for the photocatalytic coupling of 4-fluorothiophenol.

Figure S21. GC trace for the photocatalytic coupling of 4-bromothiophenol.

Figure S22. GC trace for the photocatalytic coupling of 4-tert-butylthiophenol.

Figure S23. GC trace for the photocatalytic coupling of 4-(trifluoromethyl)thiophenol.

1. General information

All chemicals used in this work were purchased from commercial supplies without further purification. Powder X-ray diffraction (PXRD) studies were carried out on a Rigaku MiniFlex 600-C diffractometer (Bragg-Brentano geometry, Cu-Ka radiation, λ= 1.54178 Å).). ^{1}H was recorded on Bruker AVANCE III 500(500 MHz).The morphologies of the samples were observed using scanning electron microscopy (SEM, Zeiss Gemini SEM 500 apparatus) with an energy-dispersive X-ray spectrometry (EDS). Samples for SEM tests were dispersed in EtOH with the aid of sonication, and then deposited on a conductive tape. Transmission electron microscopy (TEM) investigations was performed by Tecnai G2 F20 S-TWIN. Prior to TEM measurements, samples were dispersed in ethanol using a sonication method, and then mounted on a carbon coated copper grid. Fourier transform infrared (FT-IR) spectra were obtained with KBr pellets using a Bruker Tensor 27 FT-IR spectrometer. XPS analyses were performed on a Thermo Scientific ESCALAB 250Xi with a monochromatized micro-focused Al Ka X-ray source provided by eceshi (www.eceshi.com). Binding energies (BE) were calibrated by setting the measured BE of C Is to 284.65 eV. The sorption isotherms were measured with an ASAP 2460/2020 gas sorption analyzer. Inductively coupled plasma mass spectrometry (ICP-MS) was conducted on Agilent 7800. UV-vis absorption spectra were recorded on a Shimadzu UV-3600 Plus spectrometer. Fluorescence spectra were measured on an Edinburgh FLS1000 Photoluminescence Spectrometer. The products were analyzed by gas chromatograph (Agilent 8890 GC System chromatograph equipped with FID detector), and the yields of the product were determined using n-hexadecane as internal standard considering the response factors unity. The products were also characterized by GC–MS (Agilent Technologies GC-MS 5977B, Q-Exactive). The pyrene-based ligand 1,3,6,8-tetrakis(3-carboxyphenyl) pyrene (H_4PTTB) was synthesized according to our recent work.[1]

2. Experimental Section

2.1 Single Crystal X-ray Crystallography

The X-ray diffraction data was collected with a Rigaku Super Nova X-RAY diffractometer system equipped with Cu-kα radiation (λ = 1.54178 Å). The crystal was kept at 298 K during data collection. The structure was solved with the SIR2004 structure solution program integrated in Olex2 using Direct Methods, and refined with the XH refinement package using CGLS minimization.[2] The structure was solved with the ShelXS structure solution program integrated in Olex2 using Direct Methods, and refined with the ShelXL refinement package using CGLS minimization. All the solvent molecules have been removed by the SQUEEZE program.[3] The positions of the hydrogen atoms are generated geometrically. A summary of the crystal structure refinement data and selected bond angles and distances are provided in Tables S2 and S3. Crystallographic data for the structure have been deposited in the Cambridge Crystallographic Data Center with CCDC reference number 2347068.

2.2 Photoelectrochemical characterization

Photoelectrochemical measurements were performed on a CHI 660E electrochemical work station (Chenhua Instrument, Shanghai, China) in a standard three-electrode system with the photocatalyst-coated FTO, Pt plate and Ag/AgCl as the working electrode, counter electrode and reference electrode, respectively. The as-synthesized samples (5 mg) were added into Nafion (100 μL) and ethanol (4 mL) mixed solution, giving a suspension, and then working electrodes were prepared by dropping the suspension (200 μL) onto the surface of a FTO plate. The working electrodes were dried at room temperature. The photocurrent was measured using constant voltage tracking (CVT) using a 0.1 M Na_2SO_4 solution as the electrolyte. A 300 W Xe lamp ($\lambda \geq 420$ nm) was used as the light source, and a shutter was used to modulate the light and dark conditions during the test. Photo-responsive signals of the samples were measured under chopped light at 0.5 V. The electrochemical impedance spectroscopy (EIS) was performed in frequency range from 10^{-2} to 10^{4} Hz with a bias potential of 1.5 V. The Mott-Schottky measurements were performed at frequencies of 500, 1000, and 1500 Hz, respectively. Open circuit potential (OCP) measurements are carried out using a 0.1 M Na_2SO_4 solution as the electrolyte, and other test conditions are similar with the photocurrent response measurements.

2.3 KPFM Measurement

Atomic force microscopy (AFM) equipped with Kelvin probe force microscopy (KPFM) measurements were conducted at room temperature in air with an AFM (Bruker icon). Images were acquired in tapping mode with a scan rate of 0.8 Hz by a conductive MESP tips. In KPFM, electrostatic forces between sample and the tip originate from a non-contact potential difference. In the experiment, samples were dispersed in the copper conductive adhesive. Before measurements, the sample was dried at 100 °C for 2 h. In the light irradiation experiment, a 300 W Xe lamp ($\lambda \geq$ 400 nm) was used as the light source in the measurement area between the sample and the tip of the atomic force microscope.

2.4 EPR experiments

Electron paramagnetic resonance (ESR) spectra were collected from a Bruker EMXnano spectrometer at room temperature. The EPR spectra of Ni-PTTB-NB was generated from the mixing of 50 μL solution A (5 mg of Ni-PTTB and 14 mg 4-methoxythiophenol dispersed in 5 mL CH_3CN) and 50 μL solution B (50 μL of DMPO added into 0.5 mL CH_3CN), which was irradiation under visible light ($\lambda \geq 400$ nm) for 5 min. The TEMPO-h^+ adduct spectra was obtained from the mixing of 50 μL solution A (5 mg of Ni-PTTB dispersing in 5 mL CH_3CN) and 50 μL solution B (1 mg TEMPO added into 1 mL CH_3CN), which was irradiation under visible light ($\lambda \geq 400$ nm) for 5 min.

For capturing the thiyl radicals, 10 mg Ni-PTTB-NB were dispersed in a mixed solution of 5 mL acetonitrile containing 0.2 mmol 4-methoxythiophenol and 1 mmol 5, 5-dimethyl-1-pyrrolin N-oxide (DMPO), which were then subjected to ultrasonic treatment. The DMPO was used as a spin-trapping agent. The suspension is then injected into a glass capillary and placed in a glass tube in an air environment. The glass tube was placed in the microwave cavity of EPR spectrometer and was irradiated with visible light at room temperature.

Table S1. Comparation of Ni-PTTB-NB and other heterogenous catalysts over the photocatalytic coupling of thiols into disulfide.

Catalysts	Light source	Atmosphere	Time	Selectivity	Conversion (%)	Generation rate ($mmol \cdot g \cdot h^{-1}$)	Reference
Por-DETH-COF	red LEDs	O_2	1.2 h	99	89	44.5	*Chin. Chem. Lett*., **2023,** *34*,108564
MFC-CMP	blue LED	O_2	20 min	99	99	285.1	*J. Colloid Interface Sci*., **2022**, *622*, 1045–1053
Anatase-TiO_2	green LED	O_2	20 min	99	92	55.2	*Chin. J. Catal*., **2020**, *41*, 1468-1473
PdS-$ZnIn_2S_4$	$\lambda \geq 420$ nm	Ar	8 h	99	98	1.2	*Chin. J. Catal.,* **2023**, *51*, 55–65
GR-CdS-(Co-Pi)	300 W Xe lamp	Ar	5 h	99	80	1.6	*Appl. Catal. B* **2023**, *321*, 122019
PtS/$ZnIn_2S_4$	$\lambda \geq 420$ nm	N_2	6 h	99	100	1.6	*Appl. Catal. B* **2018**, *234*, 50–55
CdS/P25/Ni_2P	$\lambda \geq 400$ nm	vacuum	4.5 h	-	97	64.9	*J. Mater. Chem. A*, **2023**, *11*, 2726-2736
Bi_2S_3	blue LED	Air	6 h	99	99	3.3	*Adv. Energy Sustainability Res*. **2023**, *4*, 2300071
CdSe QDs	$\lambda > 400$ nm	-	5 h	-	86	10.3	*Angew. Chem. Int. Ed*. **2014**, *53*, 2085-2089
Ni-PTTB-NB	$\lambda > 400$ nm	Air	2 h	99	99	**8.9**	**This work**

3. Crystal Structure and Physical Characterizations of Ni-PTTB

Table S2. Crystal data and structure refinement parameters of Ni-PTTB.

Compound	**Ni-PTTB**
Formula	$C_{44}H_{16}Ni_2O_{10}$
Fw	821.99
Temp, K	298 K
Crystal system	monoclinic
Space group	C2/m
a/Å	22.0355(4)
b/Å	21.6353(4)
c/Å	17.5495(3)
α/°	90
β/°	109.5273(18)
γ/°	90
Volume/Å^3	7885.4(2)
Z	4
ρ_{calc}g/cm^3	0.692
μ, mm^{-1}	0.838
F(000)	1664
Reflections collected	33395
Independent reflections	8221
Data/restraints/parameters	8221/0/259
R_{int}	0.0365
Goodness-of-fit on F2	1.087
R1, wR2 [I>=2σ (I)]	0.0568, 0.1861
R1, wR2 [all data]	0.0597, 0.1894

Table S3. Selected bond lengths (Å) and angles (º) of Ni-PTTB

Bond Length (Å)		Bond Angle (º)	
Ni3-O	2.0935(19)	O5-Ni3-O	95.55(6)
Ni3-O5	2.0394(14)	O5[1]-Ni3-O5	89.40(10)
Ni3-O5[1]	2.0394(14)	O5[1]-Ni3-O3	88.52(6)
Ni3-O3	2.0801(19)	O5-Ni3-O1[2]	91.14(7)
Ni3-O1[2]	2.0885(14)	O5-Ni3-O1[3]	173.95(6)
Ni3-O1[3]	2.0885(14)	O3-Ni3-O	174.26(7)
Ni1-O	2.028(2)	O3-Ni3-O1[3]	85.47(5)
Ni1-O1B	1.996(2)	O1[3]-Ni3-O	90.40(5)
Ni1-O1B[1]	1.996(2)	O1[3]-Ni3-O1[2]	87.70(8)
O5-C17	1.240(2)	O1B-Ni1-O	91.32(7)
C2-C10	1.386(3)	O1B[1]-Ni1-O1B	93.70(18)
C2-C5	1.394(3)	Ni1-O-Ni3	116.02(9)
C3-C3[4]	1.439(3)	C17-O5-Ni3	130.31(15)
C3-C16	1.427(3)	C10-C2-C5	123.00(17)
C3-C14	1.419(2)	C16-C3-C3[4]	119.7(2)
C-C11	1.391(3)	C14-C3-C3[4]	119.9(2)
C-C17	1.504(3)	C14-C3-C16	120.36(16)
C-C19	1.388(3)	C11-C-C17	119.38(18)
C10-C12	1.490(3)	C19-C-C11	119.22(19)
C10-C14	1.407(2)	C19-C-C17	121.39(18)
		C2-C10-C12	118.36(16)
		C2-C10-C14	119.02(17)
		C14-C10-C12	122.60(17)
		C2-C5-C8	117.85(16)
		C2-C5-C16	118.93(17)
		C16-C5-C8	123.22(17)

Symmetry transformations used to generate equivalent atoms: [1]+X,1-Y,+Z;[2]1/2-X,1/2-Y,1-Z;[3]1/2-X,1/2+Y,1-Z;[4]1/2-X,1/2-Y,-Z

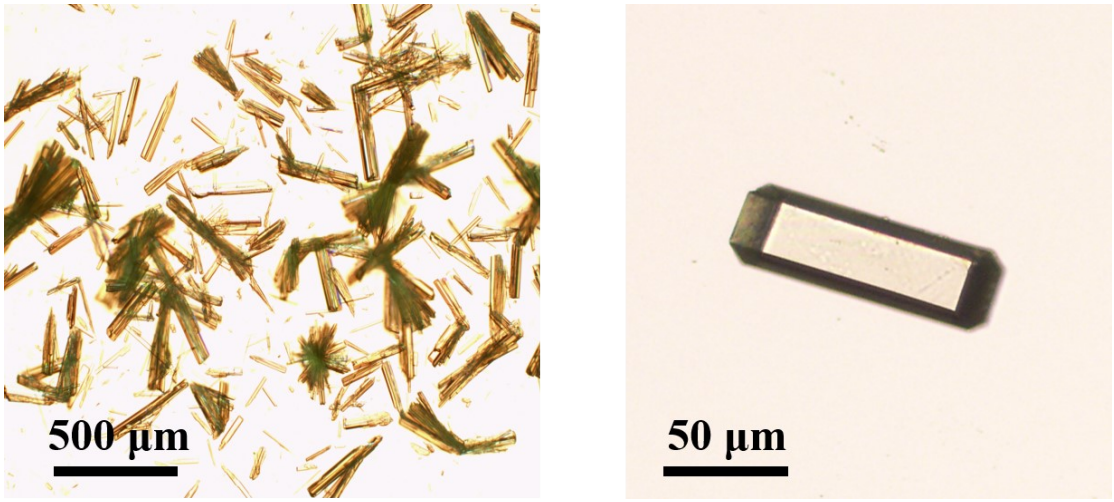

Figure S1. Optical microscope image of single crystalline Ni-PTTB

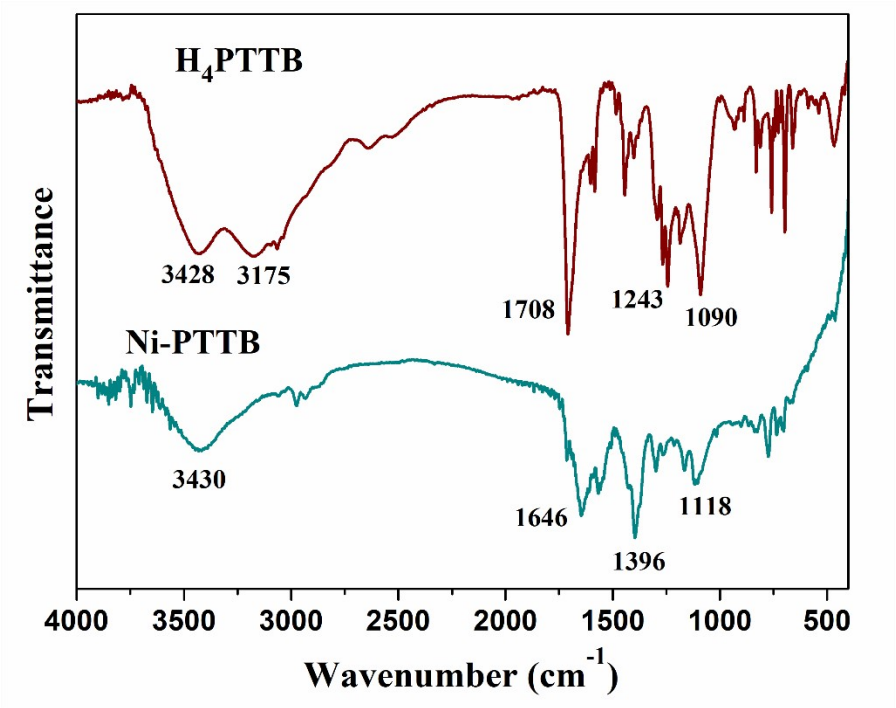

Figure S2. The FT-IR spectra of H_4PTTB and Ni-PTTB.

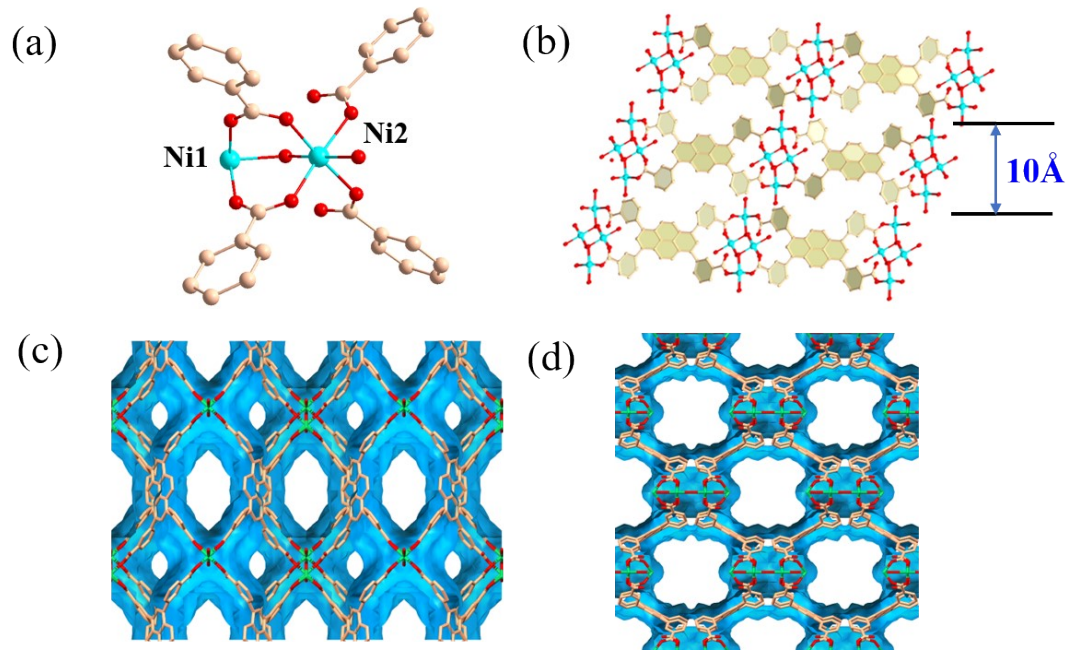

Figure S3. (a) The coordination mode of the Cd atom in Ni-PTTB; (b) The layered structure of Ni-PTTB with interlayer distance of 10 Å. Color representation: O (red); C (Tan); Cd (Turquoise). H atoms are removed for clarity. The crystal structures of Ni-PTTB viewed along the a axis (c) and c axis (d), respectively. (the external and internal pore surfaces are shown in blue)

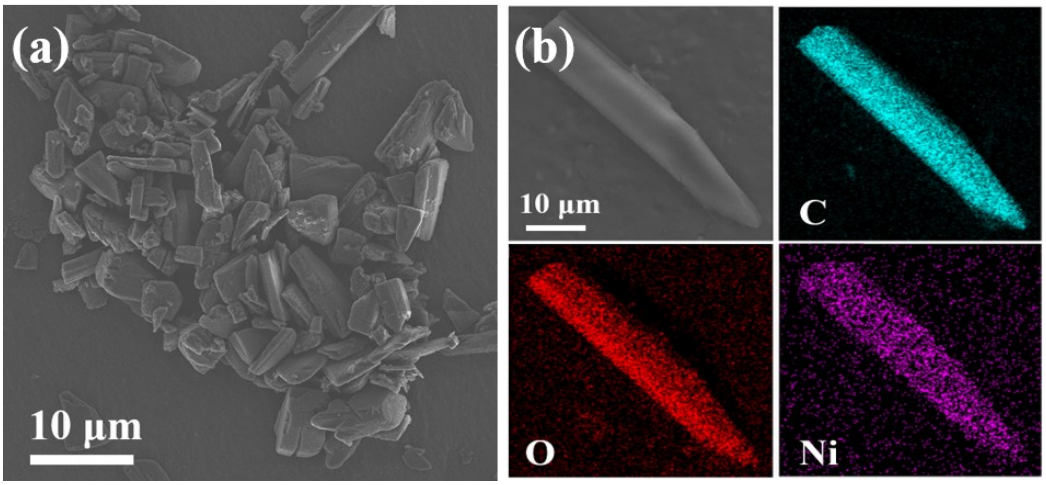

Figure S4. SEM (a) and EDS mapping images (b) of Ni-PTTB.

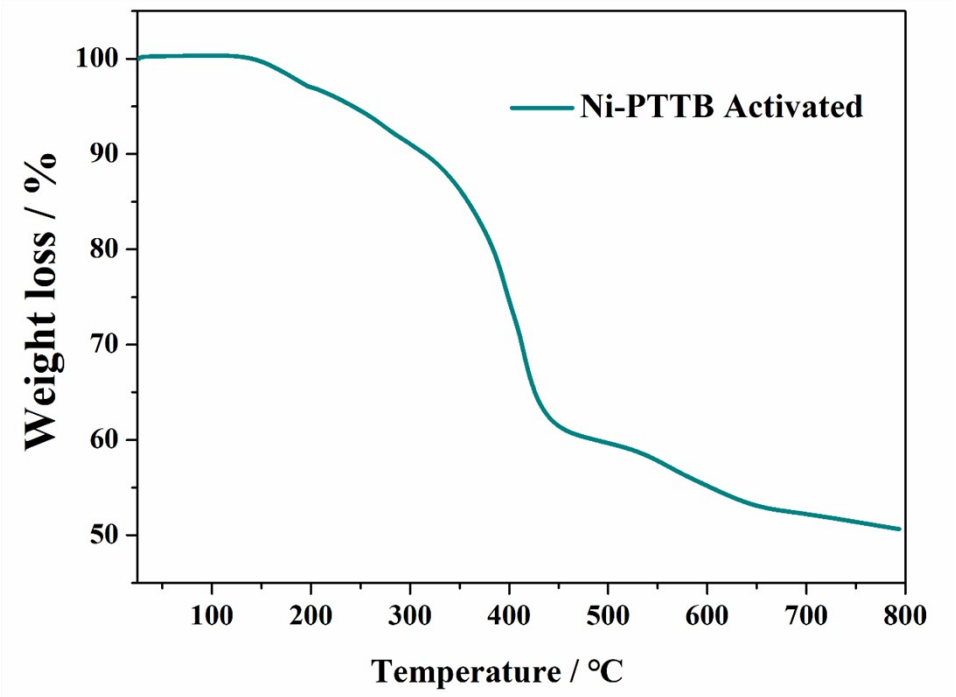

Figure S5. The TG curves of activated Ni-PTTB samples.

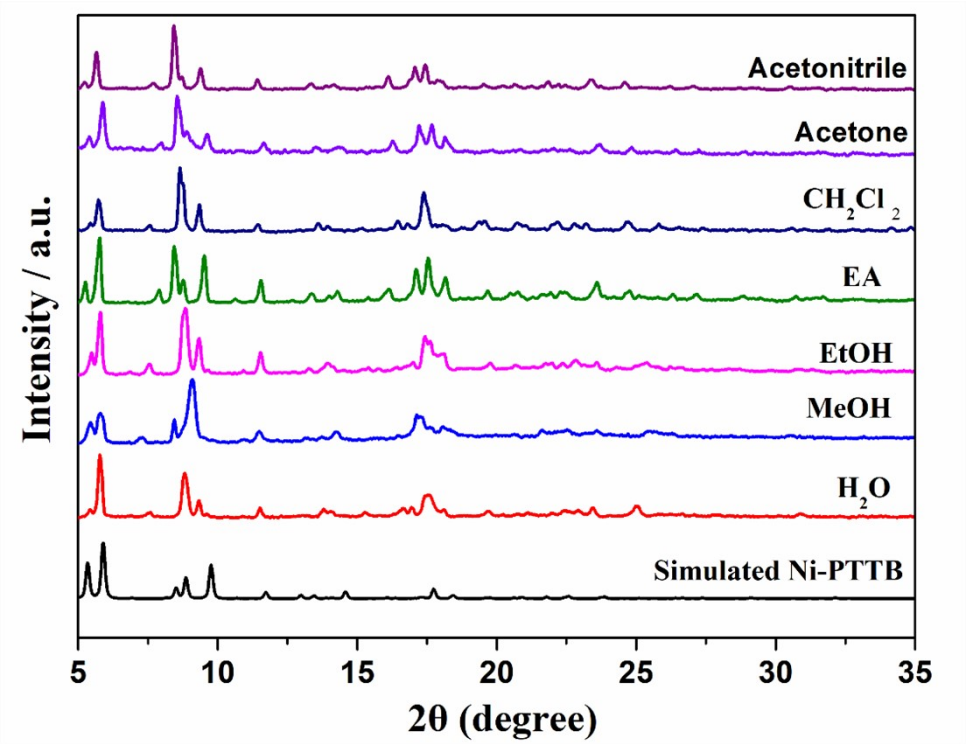

Figure S6. Stability test of Ni-PTTB in different solvents for 5 days.

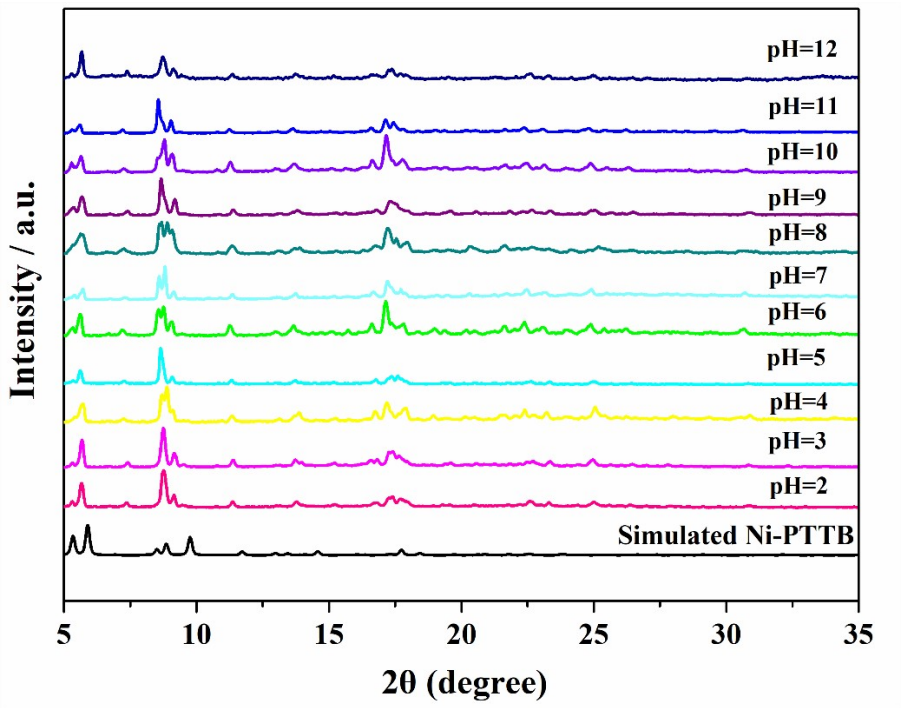

Figure S7. Stability test of Ni-PTTB in aqueous solutions with a pH range from 2 to 12 for 5 days.

4. Physical Characterizations of Ni-PTTB-NB

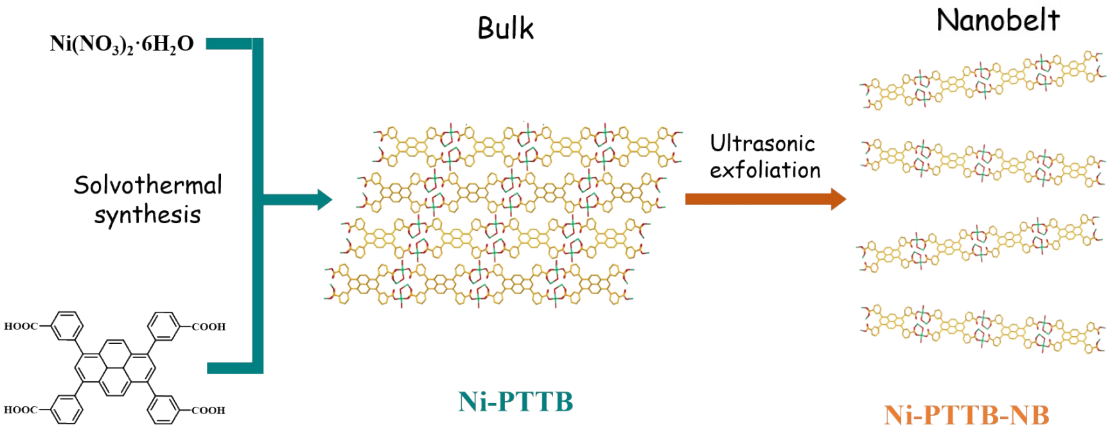

Figure S8. Schematic of synthetic route of Ni-PTTB and Ni-PTTB-NB nanobelt.

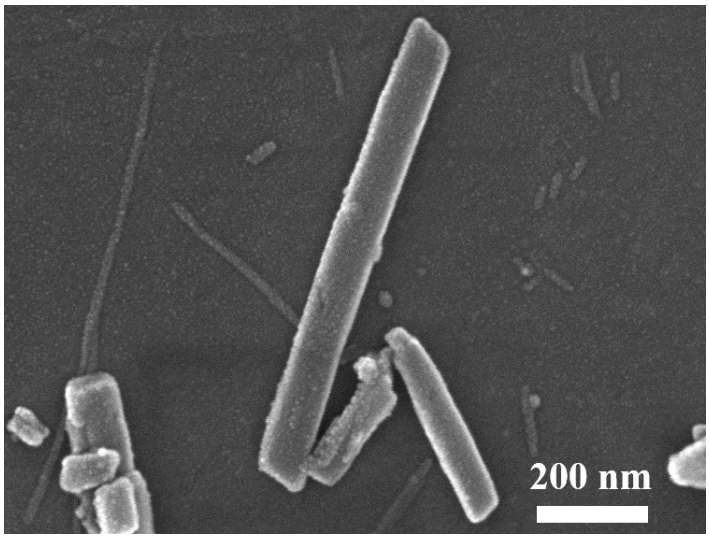

Figure S9. SEM image of 2D Ni-PTTB-NB.

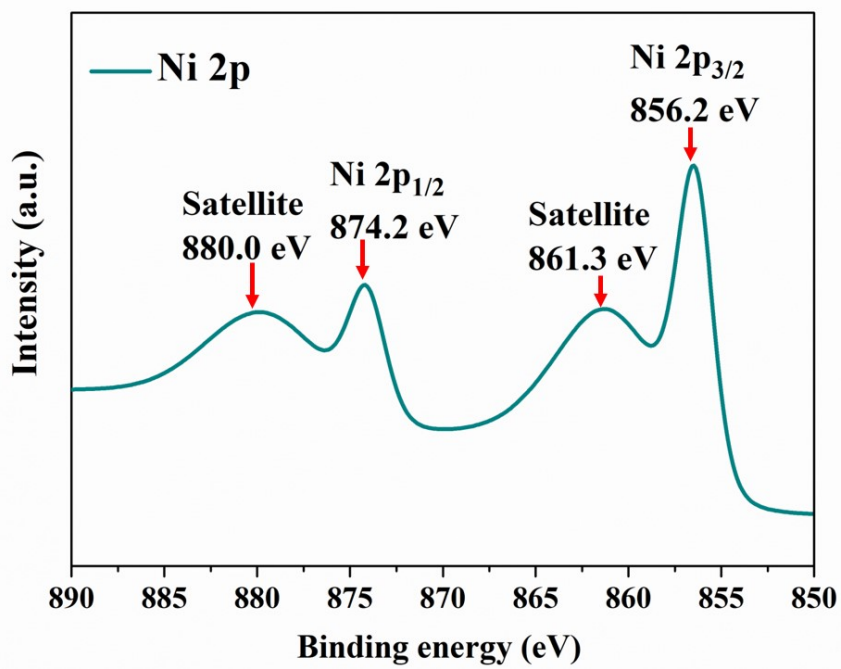

Figure S10. High resolution XPS spectra of Ni 2p in 2D Ni-PTTB-NB.

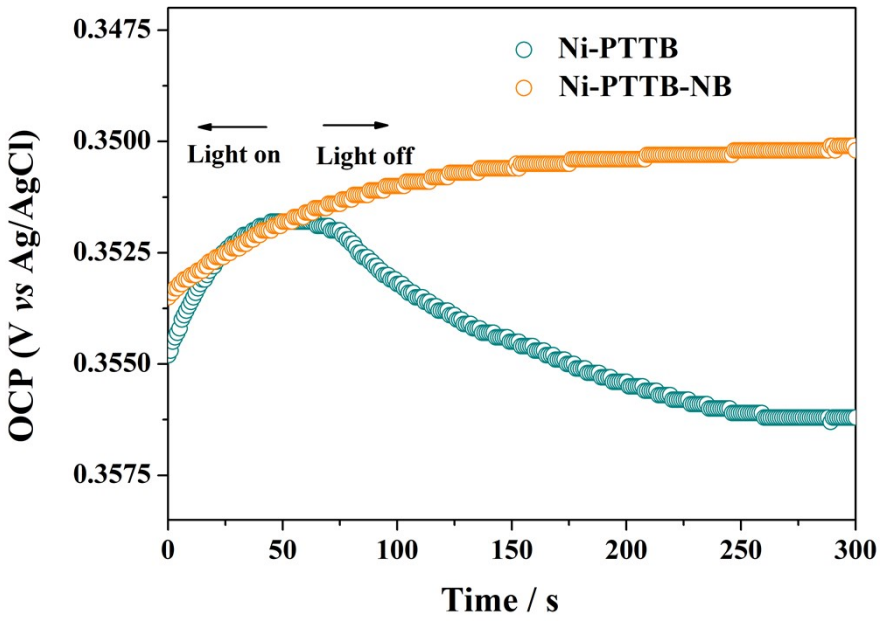

Figure S11. Open-circuit potential as a function of time under visible light for Ni-PTTB and Ni-PTTB-NB.

5. Photocatalytic Coupling of Thiols into Disulfides

Table S4. Solvent optimization for the photocatalytic coupling of thiol[a]

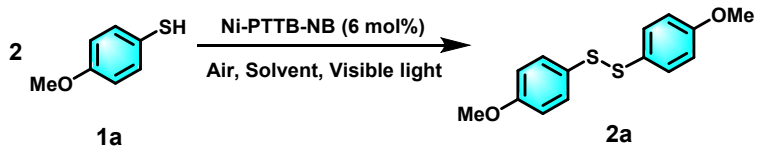

1a 2a

Entry	Solvent	Conversion (%)[b]	Selectivity (%)[c]
1	MeCN	99	99
2	n-Hexane	-	-
3	THF	trace	-
4	Ethyl acetate	trace	-
5	MeOH	58.7	99

[a] Reaction condition: 4-methoxythiophenol (14 mg, 0.1 mmol), Ni-PTTB-NB (5.6 mg, 6 mol%), solvent (5 mL), visible light ($\lambda > 400$ nm), 2 h. [b]The conversion of 4-methoxythiophenol was determined by gas chromatography (GC) using hexadecane as internal standard. [c]The selectivity of corresponding bis(4-methoxyphenyl) disulfide was determined by GC using hexadecane as internal standard.

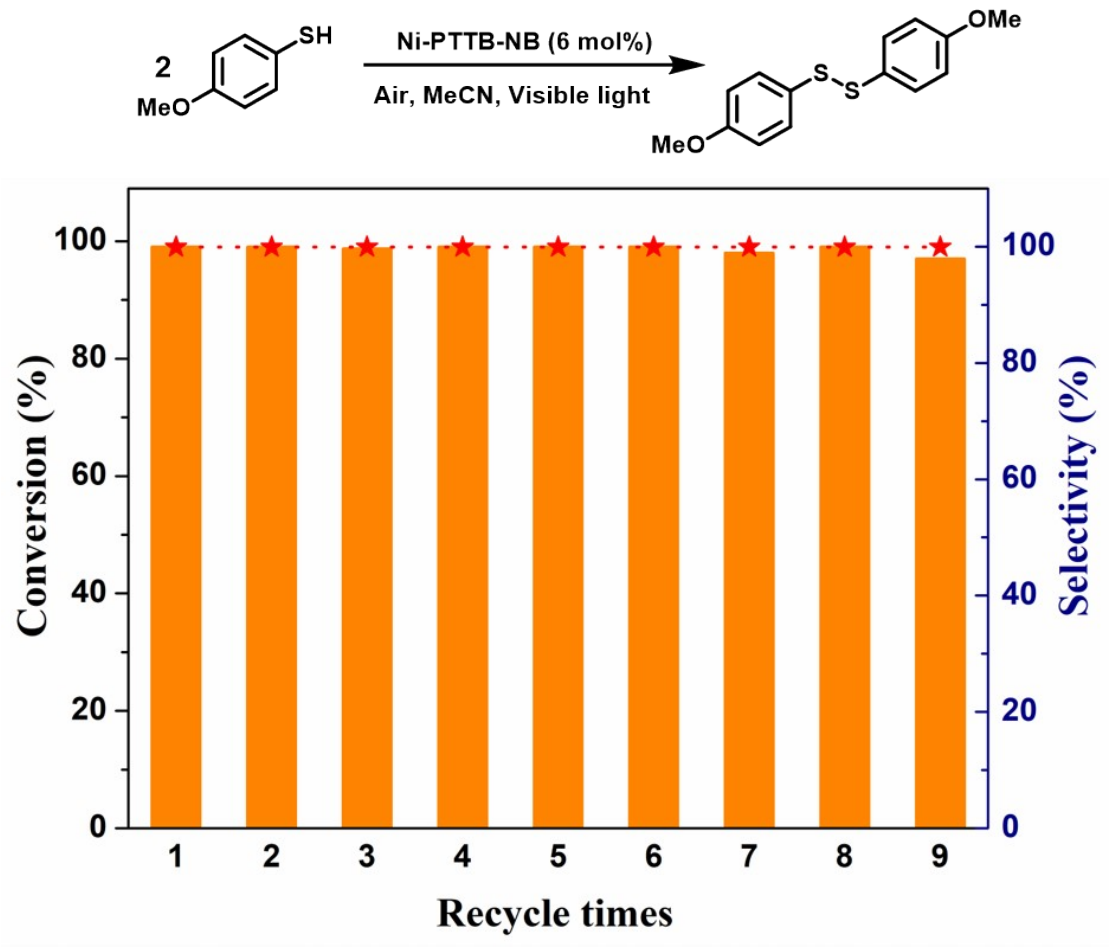

Figure S12. The recycling experiment of 2D Ni-PTTB-NB for the photocatalytic coupling of thiols to disulfide.

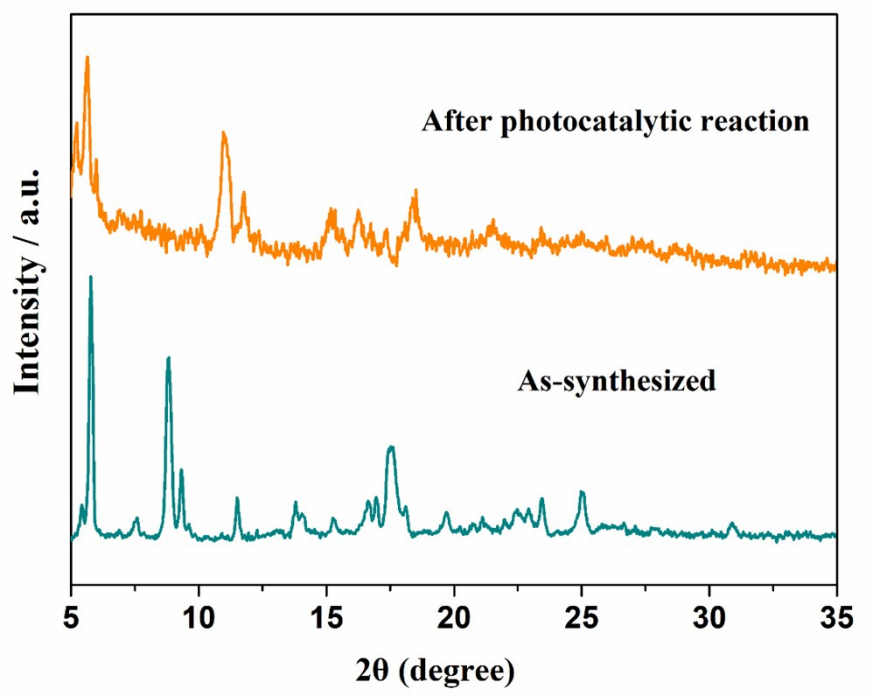

Figure S13. The PXRD patterns of 2D Ni-PTTB-NB before and after photocatalytic reaction.

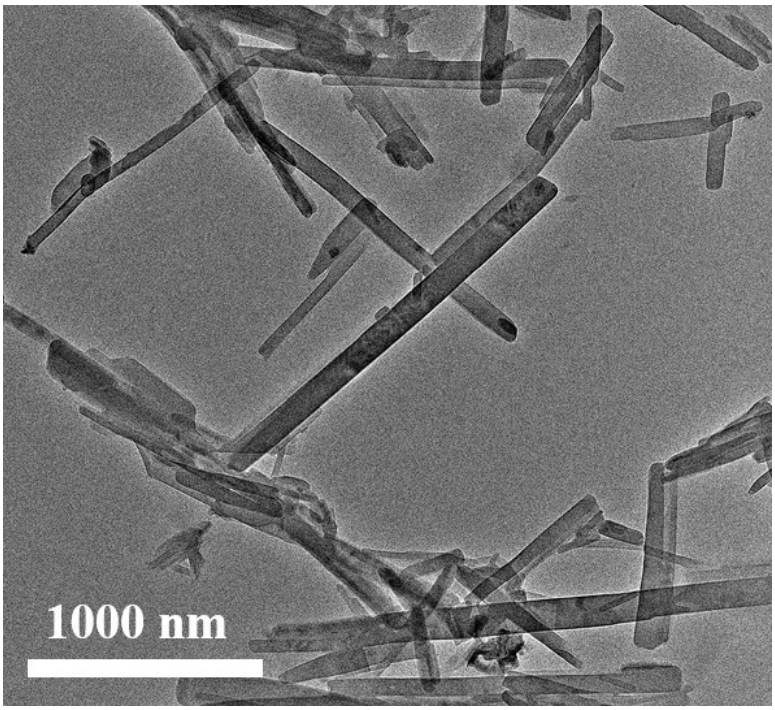

Figure S14. The TEM images of 2D Ni-PTTB-NB after photocatalytic reaction.

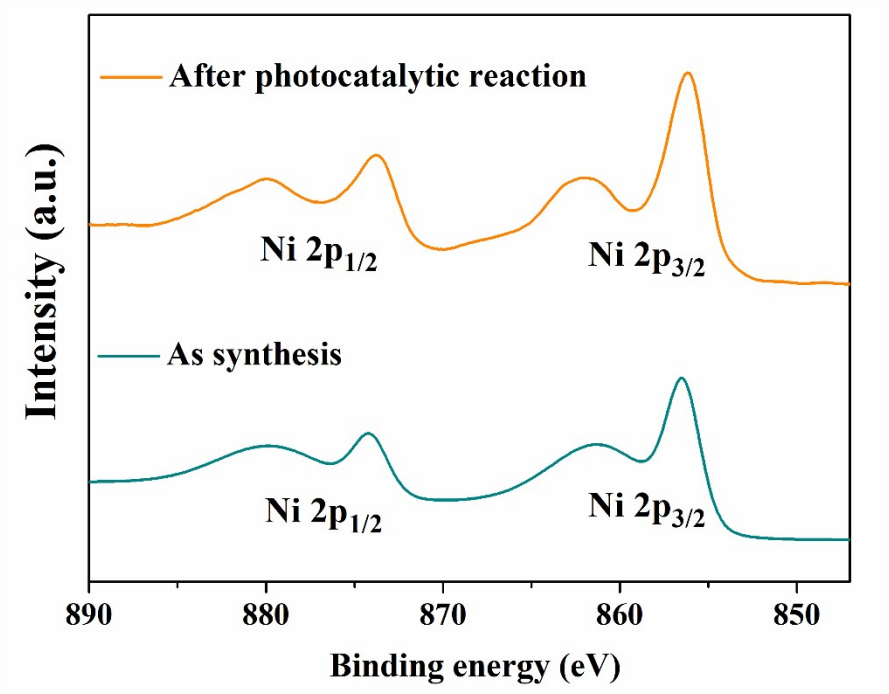

Figure S15. XPS spectrum of 2D Ni-PTTB-NB after catalytic reaction.

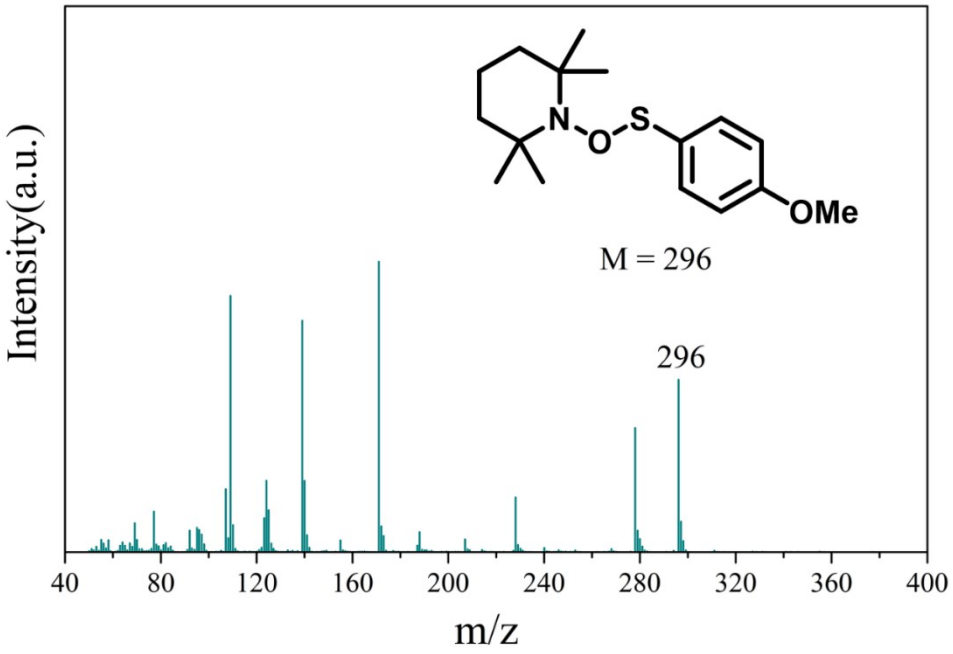

Figure S16. Trapping of thiyl radical-TEMPO adduct measured by GC-MS.

GC and GC-MS spectra of the products

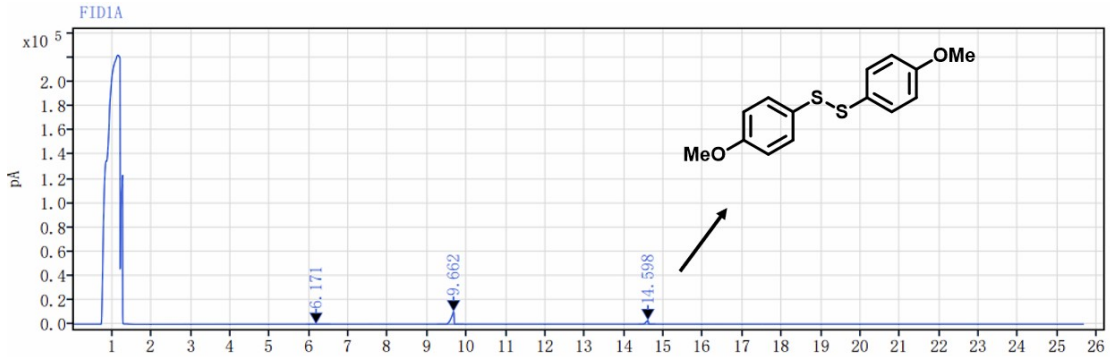

6.171	MM m	0.61	51.01	10.71	0.08
9.662	MM m	0.68	51359.78	10219.51	80.49
14.598	MM m	0.43	12395.69	3034.74	19.43

Figure S17. GC trace for the photocatalytic coupling of 4-methoxythiophenol.

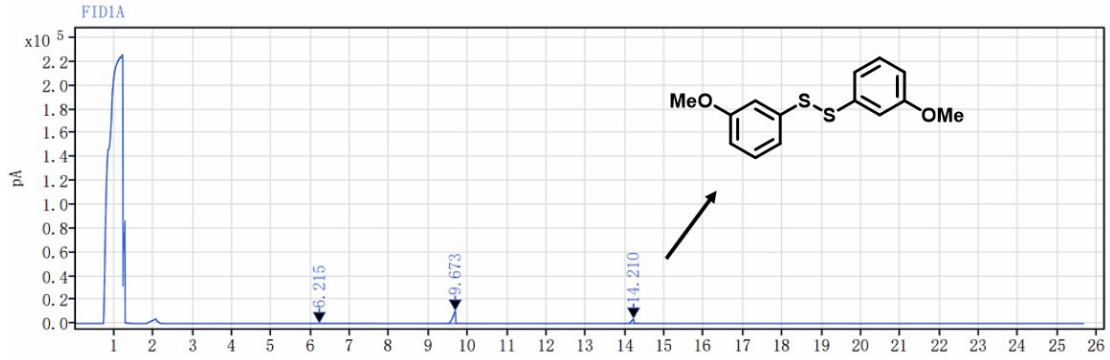

6.215	MM m	1.63	190.92	8.63	0.29
9.673	MM m	0.61	49372.63	10491.66	75.32
14.210	MM m	0.47	15984.72	3775.47	24.39

Figure S18. GC trace for the photocatalytic coupling of 3-methoxythiophenol.

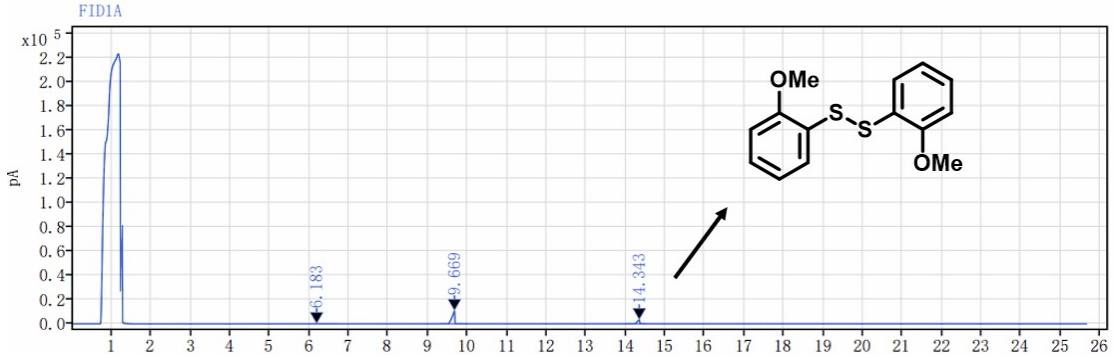

6.183	MM m	0.60	38.12	11.43	0.06
9.669	MM m	0.68	49653.94	10766.31	79.22
14.343	MM m	0.52	12989.90	3290.32	20.72

Figure S19. GC trace for the photocatalytic coupling of 2-methoxythiophenol.

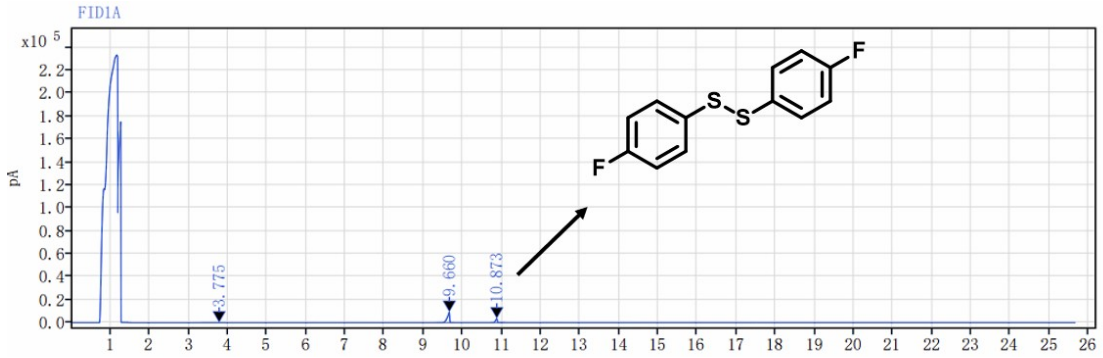

3.775	MM n	0.62	20.76	1.46	0.04
9.660	MM m	0.45	38576.73	9167.35	78.40
10.873	MM m	0.36	10607.14	3445.54	21.56

Figure S20. GC trace for the photocatalytic coupling of 4-fluorothiophenol.

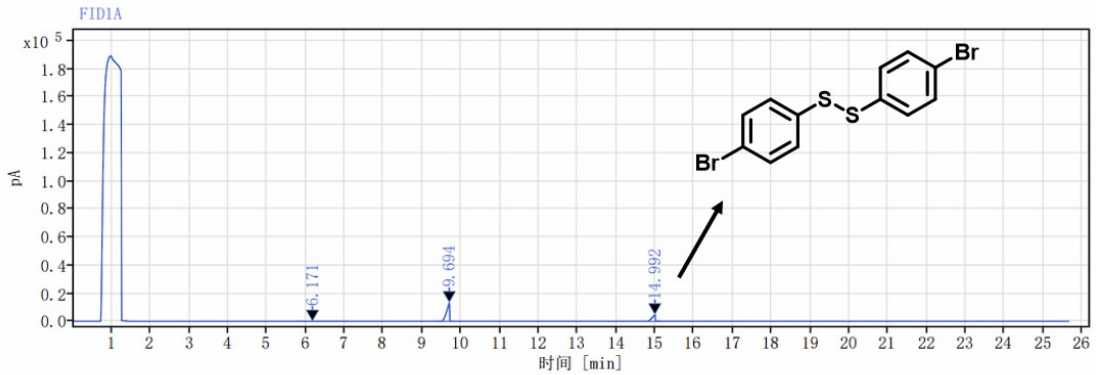

6.171	MM m	1.37	46.20	14.65	0.05
9.694	MM m	0.42	69732.55	13301.73	72.65
14.992	MM m	0.38	26199.52	4659.37	27.30

Figure S21. GC trace for the photocatalytic coupling of 4-bromothiophenol.

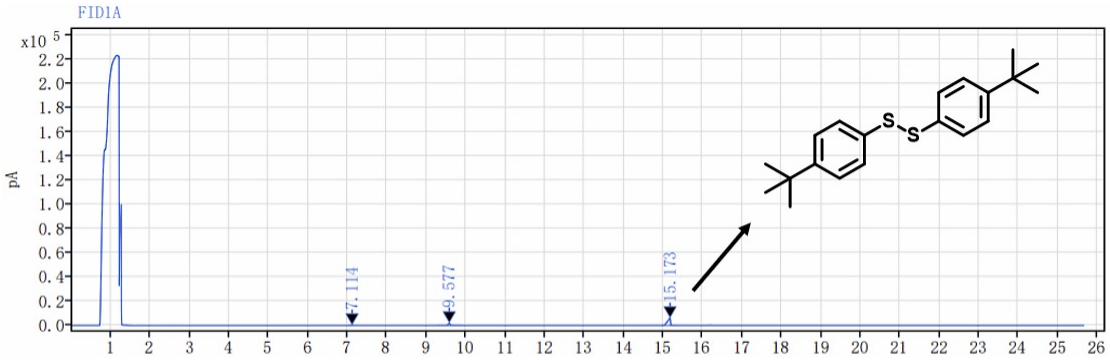

7.114	MM m	0.11	485.25	222.15	1.25
9.577	MM m	0.63	6414.32	2030.11	16.57
15.173	MM m	0.41	31805.67	6130.95	82.17

Figure S22. GC trace for the photocatalytic coupling of 4-tert-butylthiophenol.

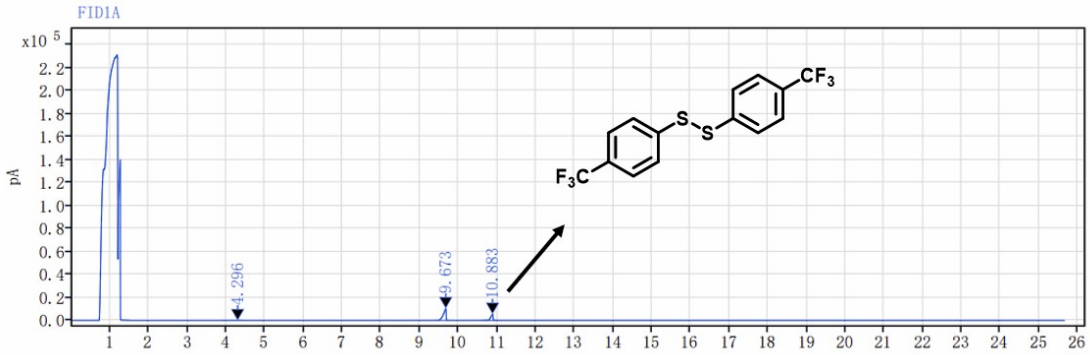

4.296	MM m	0.57	0.99	0.28	0.00
9.673	MM m	0.37	51023.30	10434.54	69.89
10.883	MM m	0.46	21984.75	5518.29	30.11

Figure S23. GC trace for the photocatalytic coupling of 4-(trifluoromethyl)thiophenol.

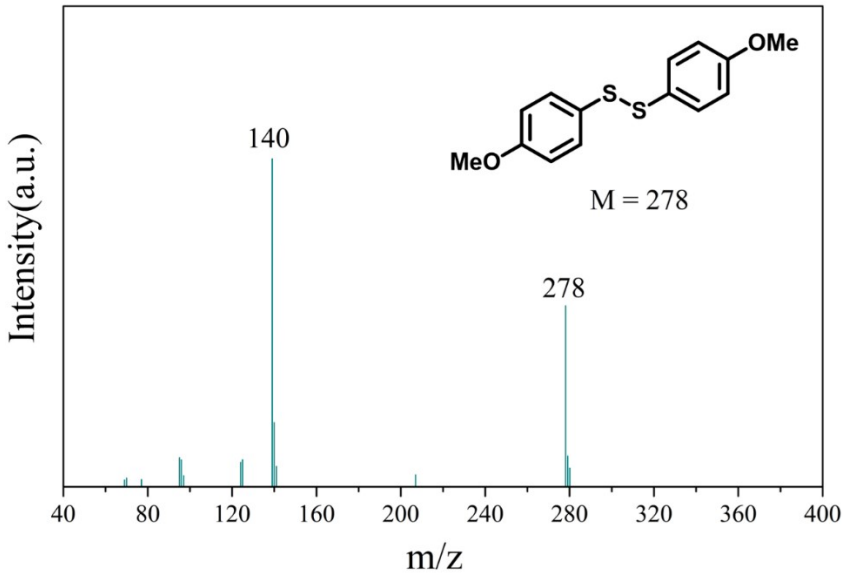

Figure S24. Mass spectra of bis(4-methoxyphenyl) disulfide measured by GC-MS.

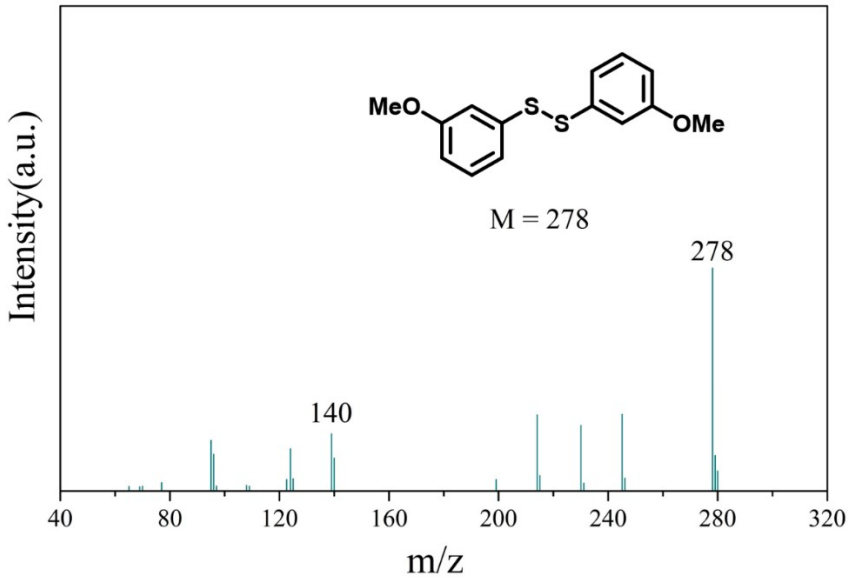

Figure S25. Mass spectra of bis(3-methoxyphenyl) disulfide measured by GC-MS.

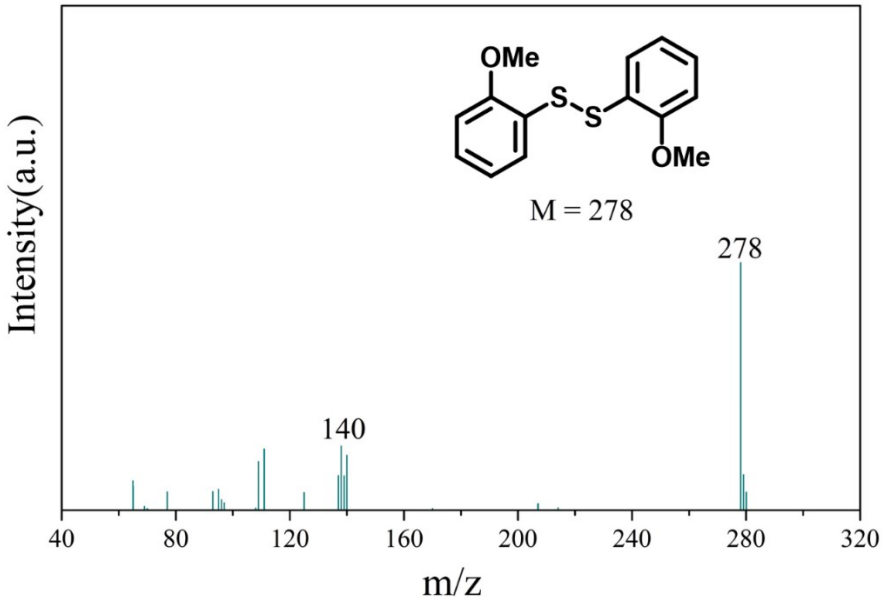

Figure S26. Mass spectra of bis(2-methoxyphenyl) disulfide measured by GC-MS.

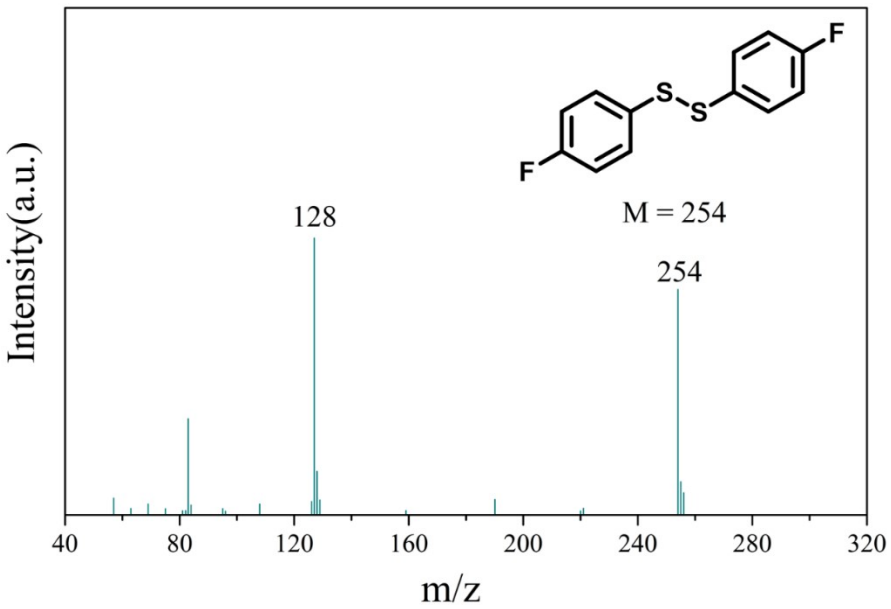

Figure S27. Mass spectra of bis(4-fluorophenyl) disulfide measured by GC-MS.

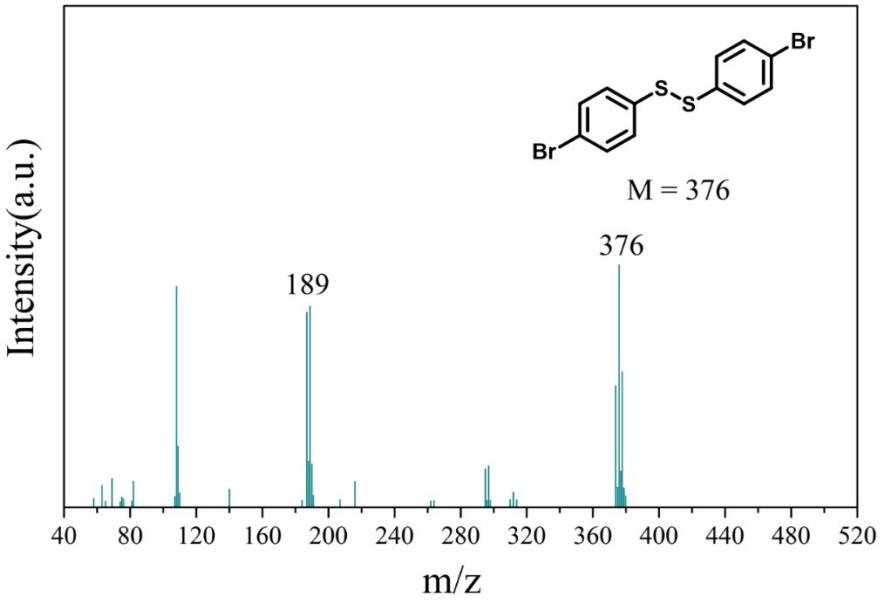

Figure S28. Mass spectra of bis(4-bromophenyl) disulfide measured by GC-MS.

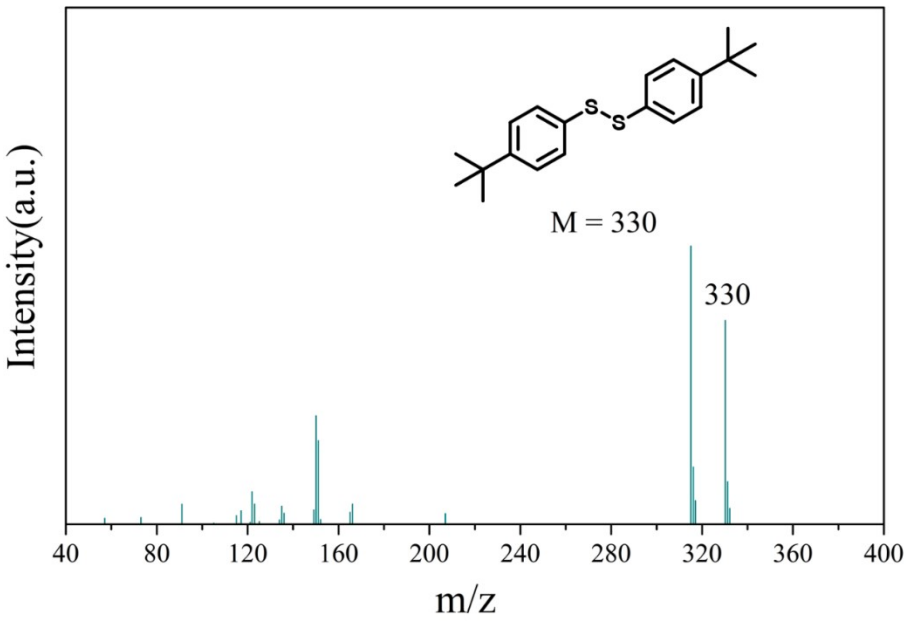

Figure S29. Mass spectra of bis(4-tert-butyl) disulfide measured by GC-MS.

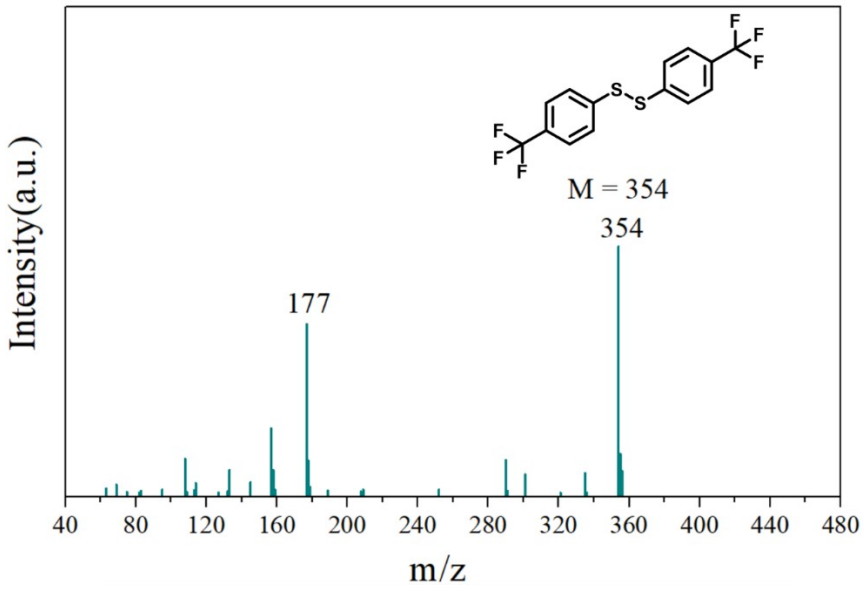

Figure S30. Mass spectra of bis(4-trifluoromethylphenyl) disulfide measured by GC-MS.

Reference

[1] Zhao, X.; Qin, B.-B.; He, T.; Wang, H.-P.; Liu, J. Stable Pyrene-Based Metal−Organic Framework for Cyclization of Propargylic Amines with CO_2 and Detection of Antibiotics in Water. *Inorg. Chem*. **2023**, *62*, 18553−18562.

[2] Sluis, P. V. D.; Spek, A. L. BYPASS. an Effective Method for the Refinement of Crystal Structures Containing Disordered Solvent Regions. *Acta Crystallogr*. **1990**, *A46*, 194−201.

[3] Dolomanov, O. V.; Bourhis, L. J.; Gildea, R. J.; Howard, J. A. K.; Puschmann, H. OLEX2: a complete structure solution, refinement and analysis program. *Appl. Crystallogr*. **2009**, *42*, 339−341.